Int. J. Solids Structures Vol. 29, No. 18, pp. 2217–2234, 1992
Printed in Great Britain.

0020–7683/92 $5.00+.00

TRANSIENT THERMAL EFFECTS IN EDGE DISLOCATION GENERATION NEAR A CRACK EDGE

L. M. BROCK
Department of Engineering Mechanics, University of Kentucky, Lexington, KY 40506, U.S.A.

(*Received* 27 *July* 1991; *in revised form* 8 *January* 1992)

Abstract—A transient 2-D study of edge dislocation generation near a crack in a fully-coupled thermoelastic solid loaded by SV-wave diffraction is considered. Exact solutions to the mixed boundary/initial value problem in the integral transform space are obtained, and inversions valid for short times performed.

The solution behavior indicates that the generation process requires only a short time period, and that thermal effects might be important. In particular, a thermally-sensitive dislocation takes longer to be emitted from the crack edge region than one described in a non-thermal analysis but, on the other hand, does not arrest.

Moreover, in contrast to the simple relaxation effect seen in non-thermal analyses, dislocation generation here causes oscillations in the dynamic stress intensity factor. Finally, the average temperature gradient across the dislocation cut is large enough to suggest that generation may be a potential source of local material disorder.

INTRODUCTION

In a series of articles, Brock (1989a,b) and Brock and Wu (1990a,b) examined the generation, or emission, of dislocations at crack edges in dynamically-loaded elastic solids. The articles complemented earlier quasi-static emission work by authors such as Rice and Thomson (1974), Majumdar and Burns (1981) and Ohr (1985). Both sets of analyses treated, variously, classical (Love, 1944) edge and screw dislocations, and cracks under Mode I, II and III loadings. The results indicated that dislocation generation can lower—if temporarily, in a transient study—the stress intensity factor, that emitted dislocations generally arrest, and that generation is more likely to occur than purely brittle fracture.

These analyses all, however, neglected thermal effects. This can perhaps be justified on the grounds that, while crack edges can exhibit pronounced thermal behavior (Weichert and Schonert, 1974; Zehnder and Rosakis, 1991), a fully plastic zone is usually present. Indeed, in a study not specific to fracture, Taylor and Quinney (1934) argued that 90% of any mechanical heat produced can be associated with plastic deformation.

On the other hand, they also noted that some of the remaining heat may be associated with dislocation motion. Moreover, Brock *et al.* (1992) and Brock and Thomas (1992) showed recently that the plastic zone near a thermally-sensitive crack edge can be quite rudimentary. Finally, dislocation motion is itself a mechanism for plastic flow (Taylor, 1934).

All this suggests that useful insight into the role of thermal effects in the dynamic response of regions near the crack edges would be gained by examining the limit case of a single dislocation moving out from an otherwise brittle crack edge in a thermoelastic solid subjected to dynamic loading. This idealized analysis would complement the non-thermal dislocation-crack interaction studies cited above. More importantly, it would focus attention closely on the thermoelastodynamic interaction of two of the basic features of fracture models—the crack edge and the dislocations that constitute an important part of its inelastic zone. The analytical results would serve as a guide in the construction of more elaborate dynamic fracture models, e.g. fully-developed inelastic zones with dislocation distributions, and outright crack propagation.

This paper, therefore, considers the generation of an edge dislocation at a crack in a 2-D thermoelastic solid subjected to dynamic loading. For simplicity, the crack is semi-infinite

and the loading is by plane SV-wave diffraction, i.e. is Mode II. The dislocation speed is constant and subcritical, after Johnston and Gilman (1959). The solid is initially at rest, and satisfies the fully-coupled linear thermoelastic equations for an isotropic, homogeneous material. The elastic constants and other mechanical properties are assumed to remain constant with temperature, after Boley and Weiner (1960) and Chadwick (1960).

The difficulties of the fully-coupled equations are mitigated somewhat because, as Brock (1989b) has shown, dislocation generation occurs in the order of microseconds after crack loading. That is, a transient analysis can legitimately treat a semi-infinite crack in an unbounded solid and, as will be seen, make use of valid approximations in obtaining the final solution expressions.

PROBLEM STATEMENT

Consider the xy-plane containing a closed slit $y = 0, x < 0$. The plane would be at rest at a completely uniform temperature were it not for the plane SV-wave

$$\mu m u_x = -\int_0^{s-mx} \sigma(t)\,dt, \quad u_y = 0; \; m = \frac{v_1}{v_2} > 1, \tag{1a,b}$$

which travels directly toward the slit. Here u_i is the i-displacement, μ is the shear modulus, v_2 is the rotational (S) wave speed, and v_1 is the classical non-thermal (Achenbach, 1973) dilatational (P) wave speed. The variable $s = v_1 x$ (time), while $\sigma(t)$ is the shear traction produced on planes a distance t behind the wave front.

At $s = 0$ the wave diffracts at the slit edge, thus producing a Mode II crack. Consequently, at $s = s_0 > 0$ an edge dislocation is generated at the crack edge, and travels along the positive x-axis. This motion and the associated rotational wave pattern are shown schematically in Fig. 1, where c is the dislocation speed non-dimensionalized by v_1. We treat c as a subcritical constant, i.e.

$$0 < c < c_R, \tag{2}$$

where c_R is the classical non-thermal (Achenbach, 1973) Rayleigh wave speed non-dimensionalized by v_1. The outer cylindrical wave front in Fig. 1 represents the diffraction-produced rotational waves, while the inner wave front represents those due to dislocation generation. As will be seen, for short times the process generates disturbances which behave approximately as classical dilatational waves. These, however, are not shown in Fig. 1.

The problem consists, therefore, of three elements—the initial rest state, the SV-wave state, and the (diffraction, dislocation generation) process occurring after $s = (0, s_0)$. To formulate the problem, we examine these elements in view of the governing field equations. From Boley and Weiner (1960), these can be written as

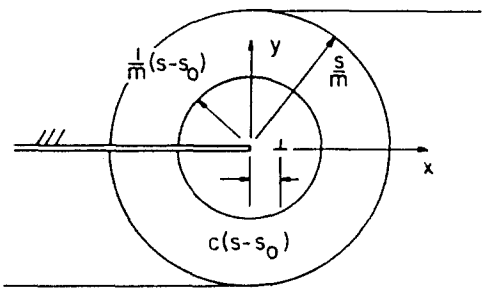

Fig. 1. Dislocation generation process and associated rotational waves.

$$[(m^2-1)\Delta+\psi\theta]_{,i}+\nabla^2 u_i-m^2\ddot{u}_i=0, \quad i=(x,y), \tag{3a}$$

$$\frac{K}{\mu}\nabla^2\theta-c_v\frac{m}{v_2}\dot{\theta}+\psi T_0 v_1\dot{\Delta}=0, \tag{3b}$$

$$\frac{1}{\mu}\sigma_{ij}=[(m^2-2)\Delta+\psi\theta]\delta_{ij}+2(u_{i,j}+u_{j,i}), \quad (i,j)=(x,y), \tag{3c}$$

where ∇^2 is the 2-D Laplacian operator, $u_i=u_i(x,y,s)$, $(\dot{\ })$ denotes s-differentiation, $(\ )_{,i}$ denotes i-differentiation, T_0 is the completely uniform initial temperature, and θ is the change in temperature from T_0. Both (T_0,θ) are measured in °K. Moreover,

$$\psi=\psi_0(4-3m^2)<0, \tag{4}$$

where ψ_0 has dimension $^\circ K^{-1}$, and (ψ_0, K, c_v) are, respectively, the coefficient of linear expansion, thermal conductivity and specific heat at constant deformation.

Equations (1) identically satisfy (3) so long as θ = constant. Because the temperature change associated with the diffraction/dislocation generation process is expected to dominate, we will take this θ to be zero. Similarly, the set $(u_i, \theta, \sigma_{ij}\equiv 0)$ satisfies (3) for a slit plane completely at rest in a uniform temperature field T_0.

Therefore, by superposition, this problem can be reduced to that of a dislocation moving for $s>s_0$ from a crack that is completely undisturbed for $s<0$ but whose faces are loaded for $s>0$ by the negative of the tractions that would be induced along $y=0$ by (1) if no crack were present. The complete solution would then be the solution for this reduced problem added to (1).

This reduced problem exhibits antisymmetry with respect to $y=0$, so that attention can be confined to the half-plane $y>0$. There, (3) holds for $s>0$ while

$$(u_i,\theta)\equiv 0, \tag{5}$$

for $s<0$. For $y=0, s>0$ we have from (1) and (3c)

$$\theta=\sigma_y=0;\ \sigma_{xy}=-\sigma(s)(x<0), \quad 2u_x=b_0H[c(s-s_0)-x]H(s-s_0)(x>0), \tag{6}$$

where H is the Heaviside function, b_0 is the Burgers vector magnitude, and a single subscript on a traction denotes repeated indices. In addition, (u_i,θ) should be continuous along elastic wavefronts, and finite as $\sqrt{(x^2+y^2)}\to\infty$ for finite s.

To solve this problem, a Wiener–Hopf (Noble, 1958) method will be used. Therefore (6) is rewritten as

$$\theta=\sigma_y=0, \quad \sigma_{xy}=-\sigma(s)H(-x)+\sigma_+(x,s)H(x)H(s-\delta x), \tag{7a,b}$$

$$2u_x=b_0H[c(s-s_0)-x]H(s-s_0)H(x)+u_-(x,s)H(-x) \tag{7c}$$

where δ is a vanishingly small, dimensionless positive constant, and

$$2u_-(0-,s)=b_0H(s-s_0). \tag{8}$$

Here (σ_+, u_-) are, respectively, the unknown shear traction σ_{xy} on the crack plane ahead $(x>0)$ of the crack edge, and the unknown u_x induced for $y=0, x<0$ by the Mode II crack surface slip. Their introduction allows conditions on all four quantities $(u_x, \theta, \sigma_{xy}, \sigma_y)$ to be stated everywhere on $y=0$. Restriction (8) recognizes that the crack surface and

dislocation-induced slips must correspond at the crack edge. The argument of the Heaviside function with σ_+ recognizes that part of the traction radiates from the crack edge as elastic waves (Achenbach, 1973) while part, satisfying the parabolic nature of (3b), establishes itself everywhere instantaneously, but probably decays exponentially for finite s as $|x| \to \infty$ (Carrier and Pearson, 1988). That is, σ_+ can be viewed as essentially zero at some time-dependent finite distance from the crack edge. It will be seen that δ does not actually appear in the solution.

TRANSFORM PROBLEM

To solve (3), (5) and (7) in view of the wavefront continuity and boundedness conditions, the unilateral and bilateral Laplace transforms

$$F = \int_0^\infty f(s)\,\mathrm{e}^{-ps}\,\mathrm{d}s, \quad F^* = \int_{-\infty}^{\infty} F(x)\,\mathrm{e}^{-pqx}\,\mathrm{d}x, \tag{9a,b}$$

(Sneddon, 1972) are introduced. Here p can be treated as real and positive, but q is, in general, complex. Application of (9) to (3) in view of boundedness/continuity and (5) gives the symmetric coupled ODE set

$$\begin{bmatrix} \partial^2 - m^2p^2a^2 & (m^2-1)pq\partial & \psi pq \\ (m^2-1)pq\partial & m^2\partial^2 - p^2b^2 & \psi\partial \\ \psi pq & \psi\partial & \dfrac{\gamma}{p}(\partial^2 + p^2q^2) - \gamma_0 \end{bmatrix} \begin{bmatrix} U_x^* \\ U_y^* \\ \Theta^* \end{bmatrix} = 0, \tag{10}$$

for $y > 0$, where ∂ denotes y-differentiation and

$$\gamma = \frac{K}{\mu v_1 T_0}, \quad \gamma_0 = \frac{c_v}{v_2^2 T_0}, \quad a = \sqrt{(1-q^2)}, \quad b = \sqrt{(m^2-q^2)}. \tag{11}$$

Here $\mathrm{Re}\,(a, b) \geqslant 0$ in the q-planes cut along $\mathrm{Im}\,(q) = 0, |\mathrm{Re}(q)| > (1, m)$. Similarly, application of (9) to (7) gives

$$\Theta^* = \Sigma_y^* = 0, \quad \Sigma_{xy}^* = \frac{\Sigma}{pq} + \Sigma_+^*, \quad U_x^* = b_0 \frac{\mathrm{e}^{-pv_0}}{2p^2(q+k)} + U^*, \quad k = \frac{1}{c}, \tag{12a-c}$$

for $y = 0$. The first term on the right-hand side of (12b) and the second term on the right-hand side of (12c) are analytic for $\mathrm{Re}\,(q) < 0$. The remaining terms in (12b,c) are analytic for, respectively, $\mathrm{Re}\,(q) > -\delta$ and $\mathrm{Re}\,(q) > -k$.

Solutions to (10) bounded for $y > 0$ are

$$U_x^* = B\,\mathrm{e}^{-pby} + x_+ A_+\,\mathrm{e}^{-pa_+ y} + x_- A_-\,\mathrm{e}^{-pa_- y}, \tag{13a}$$

$$U_y^* = \frac{q}{b} B\,\mathrm{e}^{-pby} + y_+ A_+\,\mathrm{e}^{-pa_+ y} + y_- A_-\,\mathrm{e}^{-pa_- y}, \quad \psi\Theta^* = m^2\varepsilon p(A_+\,\mathrm{e}^{-pa_+ y} + A_-\,\mathrm{e}^{-pa_- y}), \tag{13b,c}$$

which, in view of (10c) and (9), give the stress transforms

$$\frac{1}{\mu p}\Sigma_{xy}^* = -\frac{T}{b} B\,\mathrm{e}^{-pby} + X_+ A_+\,\mathrm{e}^{-pa_+ y} + X_- A_-\,\mathrm{e}^{-pa_- y}, \tag{14a}$$

$$\frac{1}{\mu p}\Sigma_y^* = -2qB\,\mathrm{e}^{-pby} + Y_+ A_+\,\mathrm{e}^{-pa_+ y} + Y_- A_-\,\mathrm{e}^{-pa_- y}. \tag{14b}$$

In (13) and (14), $(A_\pm, B)$ are as yet undetermined functions of (p, q) and

$$a_\pm = \sqrt{(M_\pm^2 - q^2)}, \quad 2M_\pm = \sqrt{\left[\left(1+\frac{1}{\sqrt{\lambda}}\right)^2 + \frac{\varepsilon}{\lambda}\right]} \pm \sqrt{\left[\left(1-\frac{1}{\sqrt{\lambda}}\right)^2 + \frac{\varepsilon}{\lambda}\right]}, \tag{15a}$$

$$(m^2 - M_\pm^2)x_\pm = q\omega_\pm, \quad a_\pm y_\pm = K_\pm + qx_\pm, \tag{15b}$$

$$X_\pm = 2qa_\pm(K_\pm - \varepsilon), \quad Y_\pm = \left(\frac{m^2 - 2M_\pm^2}{m^2 - M_\pm^2}\right)\omega_\pm + 2(\varepsilon - K_\pm)a_\pm^2, \tag{15c}$$

$$T = m^2 - 2q^2, \quad K_\pm = \gamma M_\pm^2 - 1, \quad \omega_\pm = m^2\varepsilon + (1-m^2)K_\pm, \tag{15d}$$

where

$$\lambda = hp, \quad h = \frac{\gamma}{\gamma_0}, \quad \varepsilon = \frac{1}{\gamma_0}\left(\frac{\psi}{m}\right)^2 > 0. \tag{16}$$

It can be shown that for $p > 0$, the $M_\pm$ are real and positive, with $M_+ > M_-$. Therefore, boundedness for $y > 0$ requires that $\mathrm{Re}\,(a_\pm) \geqslant 0$ in the q-plane cut along $\mathrm{Im}\,(q) = 0, |\mathrm{Re}\,(q)| > M_\pm$. In (16), h is a thermoelastic characteristic length (λ is, therefore, dimensionless), and the dimensionless parameter ε is the coupling constant (Chadwick, 1960), whose magnitude is generally $O(10^{-2})$.

Substitution of (13) and (14) into the four conditions (12) eliminates $(A_\pm, B)$ and produces an equation

$$\frac{m^2 hb}{\mu R_T}(M_-^2 - M_+^2)\left(\frac{\Sigma}{pq} + \Sigma_+^*\right) = b_0 \frac{e^{-py_0}}{2p^2(q+k)} + U_-^* \tag{17}$$

in the remaining unknowns (Σ_+^*, U_-^*), where,

$$R_T = (K_+ - \varepsilon)R_+ - (K_- - \varepsilon)R_-, \quad R_\pm = 4q^2 ba_\pm + T^2. \tag{18a,b}$$

The functions $R_\pm$ have the form of the classical Rayleigh function

$$R = 4q^2 ab + T^2, \tag{19}$$

for non-thermal solids, except the branch cuts of $a_\pm$ are—unlike those of a—functions of p. It is well known (Achenbach, 1973) that R itself has branch cuts $\mathrm{Im}\,(q) = 0, 1 < |\mathrm{Re}\,(q)| < m$ and zeroes at $q = \pm n$, where

$$n = \frac{1}{c_R} > m. \tag{20}$$

It can be shown that $(M_+ > 1, m > 1 > M_-)$ for all $p > 0$, while $m > M_+$ for all $\lambda > \lambda_0$, where

$$\lambda_0 = \frac{m^2(1+\varepsilon) - 1}{m^2(m^2-1)} \sim \frac{1}{m^2}. \tag{21}$$

Because $M_+ > M_-$ for all $p > 0$, these results indicate that the thermoelastic Rayleigh function R_T has branch cuts $\mathrm{Im}\,(q) = 0, M_- < |\mathrm{Re}\,(q)| < \max(m, M_+)$. Moreover, it is clear that $R_T(-q) = R_T(q)$ and $R_T(\bar{q}) = \bar{R}_T(q)$, where $(\bar{\ })$ denotes complex conjugate. Despite the fact that the branch cuts for R_T shift with p, the theory of the argument can

still be used to show that R_T has two real zeroes $q = \pm q_R(\lambda), q_R > \max(m, M_+)$, for all $p > 0$.

In view of this behavior and that noted earlier for the terms in (12), (17) is an equation of the Wiener–Hopf type. That is, its constituents are analytic in different regions of the q-plane. This suggests that (17) should be rewritten in such a way that the two sides are analytic in overlapping half-planes. This process is carried out in the next section; also the equation will be solved.

WIENER–HOPF SOLUTION

It can be shown that

$$R_T \sim 2\lambda(1-m^2)(M_+^2 - M_-^2)q^2 \tag{22}$$

as $|q| \to \infty$. Therefore, a function

$$G = \frac{R_T}{2\lambda(1-m^2)(M_+^2 - M_-^2)(q^2 - q_R^2)} \tag{23}$$

can be defined which has the same branch cuts as R_T but no zeroes in the cut q-plane, and approaches unity as $|q| \to \infty$. By following Noble (1958), this type of function can be factored into the product $G_+ G_-$, where the $G_\pm$ are analytic in the overlapping half-planes $\mathrm{Re}(q) > -M_-$ and $\mathrm{Re}(q) < M_+$, respectively. For the case $\lambda < \lambda_0$, these functions are given by

$$\pi \ln G_\pm = \int_M^m \frac{\Omega_1}{z \pm q}\,dz - \int_m^{M_+} \frac{\Omega_2}{z \pm q}\,dz, \tag{24a}$$

$$\Omega_1 = \tan^{-1} \frac{4z^2 b\alpha_- (K_- - \varepsilon)}{4z^2 b\alpha_+ (K_+ - \varepsilon) + \lambda(M_+^2 - M_-^2)T^2}, \tag{24b}$$

$$\Omega_2 = \tan^{-1} \frac{4z^2 \beta a_+ (K_+ - \varepsilon)}{4z^2 \beta\alpha_- (K_- - \varepsilon) + \lambda(M_+^2 - M_-^2)T^2}, \tag{24c}$$

while for $\lambda > \lambda_0$

$$\pi \ln G_+ = \int_M^{M_+} \frac{\Omega_1}{z - q_0^+}\,dZ - \int_{M_+}^m \frac{\Omega_{2+}}{z \pm q}\,dz, \tag{25a}$$

$$\Omega_{2+} = \tan^{-1} \frac{4z^2 b[\alpha_+ (K_+ - \varepsilon) - \alpha_- (K_- - \varepsilon)]}{\lambda(m_+^2 - M^2)T^2}. \tag{25b}$$

In (24) and (25), the functions $(a_\pm, b, T)$ are functions of z, and

$$\alpha_\pm = \sqrt{(z^2 - M_\pm^2)}, \quad \alpha = \sqrt{(z^2 - 1)}, \quad \beta = \sqrt{(z^2 - m^2)}. \tag{26}$$

A similar factorization can, by inspection, be obtained for b,

$$b = b_\pm, \quad b_\pm = \sqrt{(m \pm q)}, \tag{27}$$

where the $b_\pm$ are analytic in the overlapping planes $\mathrm{Re}(q) > -m$ and $\mathrm{Re}(q) < m$, respectively.

In view of these results, (17) can be rewritten as

$$\frac{m^2 b_+}{2\mu p(m^2-1)G_+(q+q_R)}\left(\frac{\Sigma}{pq}+\Sigma_+^*\right)=\frac{G_-(q-q_R)}{b_-}\left[b_0\frac{e^{-ps_0}}{2p^2(q+k)}+U_-^*\right]. \tag{28}$$

The $\Sigma_\pm^*$-term in (28) is analytic for $\mathrm{Re}(q) > -\delta$, while the $U_\pm^*$-term is analytic for $\mathrm{Re}(q) < 0$. Were it not for the poles at $q = (0, k)$, the remaining terms would also be analytic in overlapping half-planes. This suggests that they each be split into two parts by adding and subtracting the effects of the poles. The result is a rearrangement of (28) as

$$\frac{m^2 b_+ \Sigma_+^*}{2(m^2-1)pG_+(q+q_R)}+\frac{\Sigma}{2p^2 q}\frac{m^2}{m^2-1}\left[\frac{b_+}{G_+(q+q_R)}-\frac{b_+(0)}{G_+(0)q_R}\right]$$

$$+\frac{\mu b_0 e^{-ps_0}}{2p^2(q+k)}\frac{G_-(-k)(k+q_R)}{b_-(-k)}=\frac{\mu G_-(q-q_R)}{b_-}U_-^*$$

$$-\left[\frac{m^2 b_+(0)\Sigma}{2(m^2-1)p^2 qG_+(0)q_R}+\frac{\mu b_0 e^{-ps_0}}{sp^2(q+k)}\frac{G_-(q-q_R)}{b_-}+\frac{G_-(-k)(k+q_R)}{b_-(-k)}\right]. \tag{29}$$

The three terms on the left-hand side of (29) are analytic for $\mathrm{Re}(q) > -\delta$, $\mathrm{Re}(q) > -M_-$ and $\mathrm{Re}(q) > -k$, respectively, while the first two terms on the right-hand side are analytic for $\mathrm{Re}(q) < 0$, and the remaining term, for $\mathrm{Re}(q) < M_-$. Thus, the sides are analytic in the overlapping planes $\mathrm{Re}(q) > -\delta$ and $\mathrm{Re}(q) < 0$, and must be analytic continuations of the same entire function. In (29), dependence of $(G_\pm, b_\pm)$ is on q unless made explicit.

The Abelian theorems and (12c) demonstrate for $y = 0, x = 0^-$ that

$$U_x \sim \lim_{|q|\to\infty} pqU_-^* \tag{30}$$

but (8) implies that the left-hand side of (30) is $O(1)$ in q. Therefore, U_-^* must behave as $O(q^{-1})$ when $|q| \to \infty$. A check of each term shows that the right-hand side of (29) must then vanish as $|q| \to \infty$. Thus, the entire function is bounded for all q and Liouville's theorem states that such functions must be constant. Both sides of (29) are therefore, zero, and can be solved separately for (Σ_+^*, U_-^*), which essentially completes the solution of the transform problem.

Subsequent work will require σ_+, so the inversion of Σ_+^* is studied in the next section. As Achenbach (1973) and Boley and Tolins (1962) have noted, the inversion process is often the most difficult feature of coupled thermoelastic problems. As mentioned at the outset, however, our interest is primarily in short times after diffraction/generation. This provides the inversion process with some degree of simplification as will be seen later.

INVERSION OF Σ_+^*

From Sneddon (1972), the inverse operation for (9b) gives

$$\Sigma_+ = \frac{p}{2\pi i}\int_\Gamma \Sigma_+^* e^{pqx}\,dq, \quad x > 0, \tag{31}$$

where Γ can here be taken along the entire right-hand side of the $\mathrm{Im}(q)$-axis. Equation (29) yields

$$p\Sigma_+^* = -\frac{\Sigma}{q}\left[1-\frac{b_+(0)G_+(q+q_R)}{b_+G_+(0)q_R}\right]-\left(\frac{m^2-1}{m^2}\right)\frac{\mu b_0 e^{-ps_0}}{q+k}\frac{G_+(k)(k+q_R)G_+(q+q_R)}{b_+b_+(k)}, \tag{32}$$

where the relations $G_-(-q) = G_+(q)$ and $b_-(-q) = b_+(q)$ have been used. For $\mathrm{Re}\,(q) < 0$, neither the Σ- nor the b_0-terms in (32) exhibit poles, but both have the branch cuts $\mathrm{Im}\,(q) = 0, \mathrm{Re}\,(q) < -M_-$. For $x > 0$ the Cauchy theorem can be used to shift the integration from Γ onto paths around those cuts. Use of (23) avoids the need to consider the complex nature of G_+ on the cuts, and the result is that (31) and (32) give

$$2\pi\gamma(M_+^2 - M_-^2)\Sigma_+ = \frac{b_+(0)\Sigma}{(m^2-1)q_R G_+(0)} S(0,x) - \mu b_0 \frac{G_+(k)(k+q_R)}{m^2 b_+(k)} S(k,x)\,e^{-ps_0}, \tag{33a}$$

$$S(k,x) = \left[(\varepsilon - K_-)\int_M^\infty S_{1-} + (K_+ - \varepsilon)\int_{M_+}^\infty S_{1+} + \lambda(M_-^2 - M_+^2)\int_m^\infty S_m\right]\frac{e^{-pvx}}{v-k}\,dv, \tag{33b}$$

$$G_+(v+q_R)(S_{1\pm}, S_m) = \left(4v^2 b_+ \alpha_\pm, \frac{T^2}{\sqrt{(v-m)}}\right). \tag{33c}$$

Here $(G_+, b_+, \alpha_\pm)$ are functions of q, unless explicitly noted. The $S(k,x)$-integrations must be in the Cauchy principal value sense, due to the singularity at $v = k > M_-$.

To this point, the inversion process has been exact. Now, however, the Abelian theorems are invoked, which suggest that for small $(s, s-s_0)$ a transform for $p \to \infty$ $(\lambda \gg 1)$ is sufficient. For this case, $\lambda > \lambda_0$ and (26) holds. For large λ, eqns (15) show that

$$M_+ \sim 1 + \frac{\varepsilon}{2\lambda}, \quad M_- \sim \frac{1}{\sqrt{\lambda}}, \quad K_+ \sim \lambda, \quad K_- \sim -\varepsilon. \tag{34}$$

In addition, if ε is neglected in sums of the form $1 \pm \varepsilon$, then (18), (25) and (26) give

$$R_\Gamma = \lambda R + \varepsilon R_0 = 2(1-m^2)(\lambda+\varepsilon)(q^2 - q_R^2)G_+ G_-, \qquad R_0 = 4q^2\sqrt{(-q^2)}b + T^2, \tag{35a,b}$$

where use of the standard small-argument approximation $\tan^{-1}\phi \sim \phi$ allows the new definitions

$$G_\pm = F_\pm\, e^{-(\varepsilon/\lambda)D_\pm}, \qquad \pi \ln F_\pm = -\int_1^m \frac{\Omega}{z \pm q}\,dz, \quad \Omega = \tan^{-1}\frac{4z^2 b\alpha}{T^2}. \tag{36a,b}$$

We note that the relation

$$R = 2(1-m^2)(q^2 - n^2)F_+ F_- \tag{37}$$

holds, where the $F_\pm$ exhibit branch cuts for $\mathrm{Im}\,(q) = 0, -m < \mathrm{Re}\,(q) < -1$ and $\mathrm{Im}\,(q) = 0, 1 < \mathrm{Re}\,(q) < m$. Moreover, (18) and (35)–(37) demonstrate that $F_-(0) = F_+(0)$ and $G_+(0) = G_-(0)$. Therefore, setting $q = 0$ in (35)–(37) and eliminating $G_+(0)$ gives

$$n = \frac{m^2}{\sqrt{[2(m^2-1)]F_+(0)}}, \quad q_R = n\,e^{(\varepsilon/\lambda)D_+(0)}. \tag{38a,b}$$

Thus, the inverse n of the non-dimensionalized classical Rayleigh wave speed is given exactly by (38a), while (38b) provides a valid approximation for the corresponding zeroes q_R of R_Γ when p is large and $1 \pm \varepsilon$ is treated as unity. Use of all these results allows (33) to be rewritten as

$$\pi m^2 \Sigma_+ = \omega_0 \Sigma S(0,x) - \mu b_0\, e^{-ps_0 - (\varepsilon/\lambda)D_+(k)}\,\omega_k S(k,x), \tag{39a}$$

$$S(k,x) = \left[\frac{\varepsilon}{\lambda}\int_0^\infty S_1 + \int_1^\infty S_1 \alpha - \left(1 + \frac{\varepsilon}{\lambda}\right)\int_m^\infty S_m\right]\frac{e^{-pvx + (\varepsilon/\lambda)D_+}}{v-k}\,dv, \tag{39b}$$

$$(v+n)F_+(S_1,S_m)=\left(4v^2b_+,\frac{T^2}{\sqrt{(v-m)}}\right), \tag{39c}$$

where

$$\omega_0=\sqrt{\left[\frac{m}{2(m^2-1)}\right]},\quad \omega_k=\frac{(k+n)F_+(k)}{2\sqrt{(k+m)}}, \tag{40}$$

and (α, b_+, F_+, D_+) are now functions of v, if not noted otherwise. As in (33), $S(k,x)$-integrations must be performed in the Cauchy principal value sense.

The inverse unilateral Laplace transforms for terms of the form $(1/p)\,e^{\pm\phi/p}$ when $\phi>0$ are (Abramowitz and Stegun, 1964)

$$I_0[2\sqrt{(\phi s)}],\quad J_0[2\sqrt{(\phi s)}], \tag{41}$$

respectively, where (J_i, I_i) are Bessel functions and modified Bessel functions, respectively, of order i. In view of (41), the convolution theorem and the relation between the transform of a function and its s-derivative, we obtain from (39a):

$$\pi m^2\sigma_+(x,s)=\omega_0\int_0^s\sigma(s-t)S_0(t,x)\,dt-\mu h_0\omega_k S_k(s-s_0,x),\quad x>0. \tag{42}$$

Here

$$S_k(t,x)=\frac{\varepsilon}{h}\left(\int_0^t S_1 v-\int_m^t S_m\right)W_0\{2\sqrt{[\phi_k(t-vx)]}\}\frac{dv}{v-k}+\left(\int_1^t S_1\alpha-\int_m^t S_m\right)$$

$$\times\sqrt{\left(\frac{\phi_k}{t-vx}\right)}W_1\{2\sqrt{[\phi_k(t-vx)]}\}\frac{dv}{v-k}+\frac{S_1(\tau)\alpha}{x(\tau-k)}H(\tau-1)-\frac{S_m(\tau)}{x(\tau-k)}H(\tau-m), \tag{43a}$$

$$W_0=I_0(k>v),\quad J_0(k<v);\ W_1=I_1(k>v),\quad -J_1(k<v), \tag{43b}$$

$$\phi_k=\frac{\varepsilon}{h}|D_+-D_+(k)|,\quad \tau=\frac{t}{x}, \tag{43c}$$

while $S_0(t,x)$ follows by setting $k=0$ and defining

$$W_0=I_0,\quad W_1=I_1,\quad \phi_0=\frac{\varepsilon}{h}D_+. \tag{44}$$

In (41) and (42) and everywhere throughout this article, integrations vanish when the upper limit fails to exceed the lower limit. The presence of unity in these lower limits and in the Heaviside function arguments indicate that, as noted earlier, parts of the disturbances behave approximately as classical dilatational waves for short times. The presence of m, of course, signifies rotational wave disturbances, which appear for all time.

In the sequel, attention will focus on the step-stress SV-wave

$$\sigma(t)=\sigma_0H(t),\quad 0<\sigma_0\ll Y, \tag{45}$$

where Y is the yield stress. Substitution of (45) into (42) and the use of standard integral

tables (Gradshteyn and Ryzhik, 1980) gives, finally,

$$\pi m^2 \sigma_+(x,s) = \omega_0 \sigma_0 Q(s,x) - \mu b_0 \omega_k S_k(s-s_0,x), \quad x > 0, \tag{46}$$

where

$$Q(t,x) = \left(\int_0^\tau S_1 - \int_m^\tau \frac{S_m}{v} \right) \sqrt{\left(\frac{t-vx}{\phi_0} \right)} I_1\{2\sqrt{[\phi_0(t-vx)]}\}\, dv + \left(\int_1^\tau S_1 \alpha - \int_m^\tau S_m \right) I_0\{2\sqrt{[\phi_0(t-vx)]}\}\, dv. \tag{47}$$

With (46) in hand, we now examine a dislocation emission criterion.

EMISSION CRITERION

It is often held (Mura, 1982; Shaw, 1984) that dislocation motion by glide occurs when the force on the dislocation overcomes the lattice friction, a quantity that corresponds to the yield stress. This criterion has been used for both quasi-static [e.g. Rice and Thomson (1974)] and transient [e.g. Brock (1989a,b)] studies of dislocation generation. For the present Mode II case, such a criterion requires that

$$\frac{1}{b_0} F_x > Y \tag{48}$$

for generation to occur, where F_x is the dislocation force along the crack plane per unit of dislocation edge length. This force can be obtained as the gradient

$$F_x = -\frac{\partial E}{\partial \xi}, \quad E = \tfrac{1}{2} b_0 \int_\xi^\infty \sigma_{xy}(x,0,s)\, dx, \quad \sigma_{xy}(x,0,s) = \sigma_0 + \sigma_+(x,s) \tag{49}$$

of the interaction energy with respect to the dislocation position $x = \xi$ on the glide plane. Here, $\xi = c(s-s_0), s \geqslant s_0$. Substitution of (46) into (49) yields integrations that, with the exception of the non-integral functions in (43a), can be carried out by simple changes of integration order and the use of standard tables. Because of the singularity at $\tau = k$, the non-integral functions give terms that are unbounded, but such terms do not, strictly speaking, contribute to the derivative of E with respect to ξ. For the present dynamic case, however, the differentiation process must recognize that $k = 1/c$ and $c(s-s_0)$ both appear in E. In any event, the result is

$$\frac{1}{b_0} F_x = \sigma_0 + \frac{\omega_0 \sigma_0}{\pi m^2} S_a(s) - \mu \frac{b_0 \omega_k}{\pi m^2} S_b(s-s_0) - \mu \frac{b_0 S}{4\pi c(s-s_0)} \tag{50}$$

where

$$S_a(t) = \frac{\varepsilon}{h} \sqrt{(ct)} \left(\int_0^k S_1 - \int_m^k \frac{S_m}{v} \right) \sqrt{\left(\frac{k-v}{\phi_0} \right)} I_1\{2\sqrt{[\phi_0 t(k-v)]}\}\, dv + \left(\int_1^k S_1 \alpha - \int_m^k S_m \right) I_0\{2\sqrt{[\phi_0 t(k-v)]}\} \frac{dv}{v}, \tag{51a}$$

$$S_b(t) = \frac{\varepsilon}{h} \left(\int_0^k S_1 v - \int_m^k S_m \right) I_0\{2\sqrt{[\phi_k t(k-v)]}\}\, dv + \frac{1}{\sqrt{(ct)}} \left(\int_1^k S_1 \alpha - \int_m^k S_m \right) \sqrt{\left(\frac{Q_k}{k-v} \right)} I_1\{2\sqrt{[\phi_k t(k-v)]}\}\, dv \tag{51b}$$

$$S=\frac{2k}{m^2}\left(\frac{T^2}{\beta^3}+8\frac{T}{\beta}+4\frac{3k^2-2}{\alpha}\right)+\frac{2}{m^2}\left(\frac{T^2}{\beta}-4k^2\alpha\right)\left[\frac{1}{2(k+m)}-\frac{1}{k+n}-\frac{1}{\pi}\int_1^m\frac{\Omega}{(z+k)^2}\,dz\right] \tag{51c}$$

and (α, β, T) are functions of k in (51c). It should be noted that this S is identical in form to the corresponding term in the non-thermal case (Brock, 1989b).

As noted at the outset non-thermal results predict very short times between diffraction and emission. We assume the same property here, as embodied in the statement

$$d \ll s_0, \quad d = c(s-s_0). \tag{52}$$

That is, the distance traveled by the dislocation after emission is much smaller than the distance traveled by a classical dilatational wave during the diffraction–emission interval. In view of (52), a valid approximation for (50) is possible, and (48) then gives

$$\frac{1}{\mu b_0}F_x=\frac{\sigma_0}{\mu}+\frac{2}{\pi}\frac{\sigma_0}{\mu m\omega_0}\left[\sqrt{\left(\frac{s_0}{d}\right)}+\frac{4}{3(m^2-1)}\frac{\varepsilon c s_0}{h}\right]+\frac{1}{4\pi}\frac{b_0}{h}\varepsilon c S_\varepsilon-\frac{1}{4\pi}\frac{b_0}{d}S>\frac{Y}{\mu}, \tag{53}$$

where

$$m^2 c S_\varepsilon=\omega_k\left[2\int_1^k S_1 D_k\alpha-\int_0^k S_1+\int_m^k S_m\left(\frac{1}{v}-2D_k\right)\right]dv, \tag{54a}$$

$$\pi D_k=\left(\int_0^1\frac{1}{R}+\int_1^m\frac{1}{T^2}\right)\frac{4z^3 b\,dz}{(z+k)(z+v)}. \tag{54b}$$

In deriving (53), expressions for modified Bessel functions of smaller arguments have been used (Gradshteyn and Ryzhik, 1980).

The relation (53) can be viewed as a formula of second degree in $\sqrt{d}$. For a wide range of acceptable (ε, m)-values and c in the range (2), it appears that $(S, S_\varepsilon) > 0$, as shown in Fig. 2. Therefore, the form of the left-hand side of (53) suggests either of the two schematics in Fig. 3, i.e. a function F_x of $\sqrt{d}$ that becomes negative and unbounded when $d \to 0$, but increases as d grows, and approaches a positive constant value as $d \to \infty$. In case (a) the function peaks above its asymptotic value at a finite d, in case (b) the asymptotic value is the peak.

When emission for either case occurs, the peak value exceeds Y/μ. In case (a), then, two values of d would exist at which F_x drops below Y/μ. The smaller value would be the distance from the crack edge at which emission initiates and cannot, therefore, exceed the

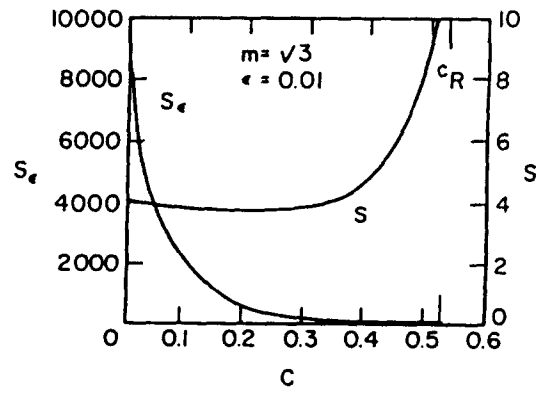

Fig. 2. Plots of S and S_ε versus dimensionless dislocation speed.

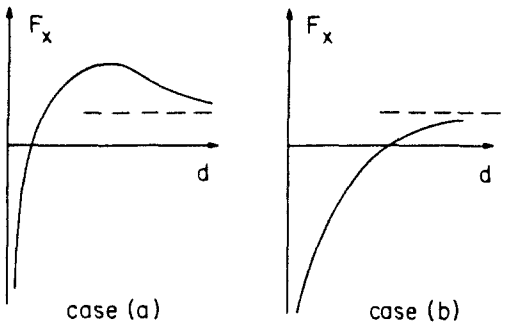

Fig. 3. Two schematics for dislocation force versus emission distance.

dislocation core radius r_c (Rice and Thomson, 1974). The larger value of d would be the distance at which the emitted dislocation stops—the present analysis would then, of course, cease to be valid. In the limit that the function peak just equals Y/μ, the two values would be the same, signifying that the dislocation is generated, but not emitted.

For emission in case (b), only one value of d would exist, signifying that the dislocation, if emitted, never stops. Before actually examining these possibilities, it is useful to compare (53) with its non-thermal counterpart.

The function given by Brock (1989b) shows two differences with (53): there are, of course, no ε-factored thermal terms, but there is no lone σ_0-term either. Strictly speaking, this term should also appear in the non-thermal result, but is dropped because $\sigma_0 \ll Y$ and the only other terms in the force are inversely proportional to $\sqrt{d}$ and d. In (53) the ε-terms do not depend on d and are, therefore, included.

Clearly, then, the non-thermal force is described by case (a), and the additional terms in (53) serve as a relaxation mechanism. That is, they could be placed on the right-hand side of (53), thereby lowering, in effect, the lattice friction that a non-thermal dislocation "sees".

In view of this discussion, we make (53) an equality and, upon multiplying through by d, obtain a quadratic equation in $\sqrt{d}$. Because the smaller (or only) root, $d = d_0$, cannot exceed r_c, we follow Brock (1989a) and require that

$$d_0 = vr_c (0 < v < 1). \tag{55}$$

Substitution of (55) back into the equation resulting from (53) then gives a relation for the emission instant s_0:

$$\sqrt{\left(\frac{s_0}{vr_c}\right)} = \frac{\mu m \omega_0}{4\sigma_0} \frac{N}{1+\sqrt{\left[1+\dfrac{4\varepsilon c \mu m \omega_0 v r_c}{6(m^2-1)\sigma_0 h} N\right]}}, \quad N = \frac{4\pi}{\mu}(Y-\sigma_0) + \frac{b_0}{h}\left(\frac{hS}{vr_c} - \varepsilon c S_\varepsilon\right). \tag{56a,b}$$

Substitution of (56) into the expression for any larger root would then give the stopping distance.

SOME CALCULATIONS

To illustrate this discussion, we assume for (2) some material properties:

$$\frac{Y}{\mu} = 0.001, \quad m = \sqrt{3}, \quad h = 0.0167\mu m, \quad \varepsilon = 0.01, \quad b_0 = 0.0001\mu m, \quad \frac{b_0}{r_c} = 0.5, \quad v = 1.0, \tag{57}$$

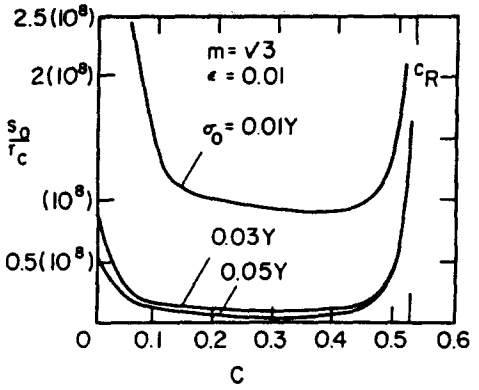

Fig. 4. Emission times versus dimensionless dislocation speed.

valid (Brock and Wu, 1990b; Brock *et al.*, 1992) at room temperature ($T_0 = 293$ °K), and consider the range

$$0 < \sigma_0 < 0.1\,Y. \tag{58}$$

For the choice of m, (38a) gives $n \sim 1.8839$. For these parameters, we find that (53) is governed by case (b). That is, generation occurs, and the emitted dislocation does not stop—at least in the short time frame of this analysis. This is in contrast to the case of (a)-governed non-thermal results, and confirms the aforementioned thermally-induced lattice fraction relaxation effect.

Plots of s_0/r_c vs c for various values of σ_0/μ are shown in Fig. 4. There, s_0 achieves minima for finite values of c, a phenomenon that also occurs in the non-thermal case, as shown by data in Fig. 5. This data is taken from Brock and Wu (1990b), who found that this behavior was in contrast to the monotonic increase in s_0 with c seen in Mode I and Mode III cases. Thus, Mode II seems to have a distinctive preference, in the sense of minimum emission time, for a specific emission speed. Data from the present analysis is also displayed in Fig. 5 for $m = 2.03$ and $\sigma_0 = 0.1\,Y$, and illustrates that s_0 generally increases when thermal effects are included. That is, a thermally-sensitive dislocation will take longer to generate, but will then move without stopping.

A return to the (S, S_ε)-plots of Fig. 2 shows more clearly, in view of (53), why case (b) governs this analysis, and why thermally-sensitive dislocations do not stop: because S_ε is $O(10^2) - O(10^3)$, the asymptotic value of the force,

$$\frac{1}{\mu b_0}(F_x)_\infty = \frac{\sigma_0}{\mu} + \frac{8\sigma_0}{\pi\mu m\omega_0}\frac{\varepsilon c s_0}{(m^2-1)h} + \frac{1}{4\pi}\frac{b_0}{h}\varepsilon c S_\varepsilon \tag{59}$$

will almost always exceed Y/μ, even if s_0 were to vanish.

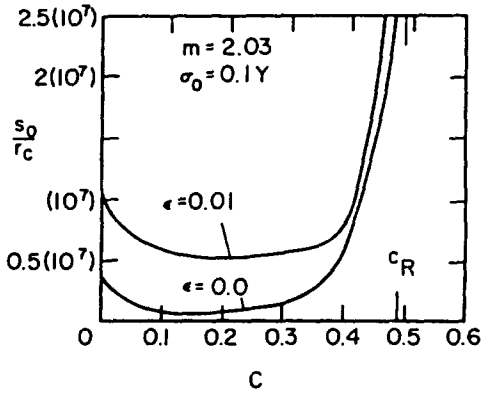

Fig. 5. Emission times for thermal and non-thermal ($\varepsilon = 0$) analyses.

With the emission possibilities examined, we now look briefly at a solution feature of interest in fracture mechanics.

DYNAMIC STRESS INTENSITY FACTOR

The Mode II dynamic stress intensity factor k_{II} can be obtained as

$$k_{II} = \lim_{x \to 0+} \sqrt{(2\pi x)}\sigma_{xy}(x, 0, s), \quad \sigma_{xy}(x, 0, s) = \sigma_0 + \sigma_+(x, s). \tag{60}$$

From (46), then, it is easy to show that

$$\frac{1}{2}\sqrt{\left(\frac{\pi}{2}\right)}k_{II} = \frac{\sigma_0}{m\omega_0}\sqrt{(s-\mu b_0)}\left(\frac{m^2-1}{m^2}\right)\frac{\omega_k}{\sqrt{(s-s_0)}}\cos\{2\sqrt{[\phi_0(k)(s-s_0)]}\}H(s-s_0) \tag{61}$$

for short times after diffraction. Comparison of (61) with the corresponding non-thermal results (Brock and Wu, 1990b) shows that the thermal effect on k_{II} does not seem to be as profound as on F_x. However, F_x in (53) is valid *near* the crack edge, where d is not necessarily negligible compared to h, while k_{II} arises from (60). Moreover, Fig. 4 indicates that the cosine function argument need not lie in the range $(0, \pi/2)$. The emission-induced contribution would then produce oscillations for $s > s_0$, thereby alternatively relaxing and enhancing k_{II}. Oscillatory behavior arises in the non-thermal case only when the loading itself is oscillatory, e.g. sinusoidal (Brock and Wu, 1990b).

Although a maximum k_{II}-based fracture criterion is seldom used, (61) can give insight into the role of thermally-sensitive dislocation emission in an intensity factor-based fracture criterion: if purely brittle Mode II fracture is assumed to initiate when k_{II} reaches a critical value, k_{II}^c, then the first term in (61) must reach that value at $s = s_c < s_0$, where

$$\frac{s_c}{r_c} = \frac{\pi}{2}\left(\frac{mY}{2\sigma_0}\omega_0 k_c\right)^2, \quad k_c = \frac{k_{II}^c}{Y\sqrt{r_c}}. \tag{62}$$

For the material described by (57),

$$k_c = 3(10^3) \tag{63}$$

is a typical value, so that when $\sigma_0 = 0.1Y$,

$$\frac{s_c}{r_c} = 4.6(10^8). \tag{64}$$

Comparison of (64) with data in Figs 4 and 5 shows that $s_c/s_0 = O(10)$. Thus, both thermal and non-thermal dislocation emission would occur before purely brittle fracture. It should at this point be noted that the k_c-value in (63) was also used by Brock and Wu (1990b), but was erroneously printed as "30" in their eqn (10.4).

AVERAGE HEAT FLUX ACROSS DISLOCATION CUT

The neglect of any SV-wave induced temperature rise θ and the resulting antisymmetry of the reduced problem means that θ vanishes along the glide plane. However, this also essentially guarantees that a heat flux due to a gradient $\partial\theta/\partial y$ will exist across the dislocation cut. For insight into this flux, we examine the average of $\partial\theta/\partial y$ over the glide plane

$y = 0, 0 < x < c(s-s_0), s \geqslant s_0$. From the transform (13c):

$$\psi \hat{c} \Theta^* = -m^2 \varepsilon p^2 (a_+ A_+ + a_- A_-) \tag{65}$$

for $y = 0$, where, from the same process that gave us (17), we find

$$A_- = -A_+, \quad A_+ = \frac{2qb}{\mu p R_T} \left(\frac{\Sigma}{pq} + \Sigma_+^* \right). \tag{66}$$

The term in parentheses can be found in (32), whereupon substitution of (65) into an inversion formula analogous to (31) and use of the large-p approximations and the integration/inversion scheme employed earlier gives

$$\frac{\pi h}{2\varepsilon} \psi \frac{\partial \theta}{\partial y} = -\frac{2}{\mu} \omega_0 \int_0^t \sigma(s-t) S_0(t, x)\, \mathrm{d}t + b_0 \omega_k S_k(s-s_0, x) \tag{67}$$

for $y = 0$, $(x, s) > 0$. Here (33b,c) hold, while (39c) and (43a) are replaced by

$$S_k(t, x) = \left(\int_0^t v - \int_1^t \alpha \right)_1 \sqrt{\left(\frac{\phi_k}{t - vx} \right)} W_1 \{ 2\sqrt{[\phi_k (t - vx)]} \} \frac{v\, \mathrm{d}v}{v - k}$$

$$+ \frac{S_1(\tau)\tau^2}{x(\tau - k)} - \frac{S_1(\tau)\tau\alpha}{x(\tau - k)} H(\tau - 1), \tag{68a}$$

$$(v + n) F_+ S_1 = b_+ \tag{68b}$$

and S_0 is obtained by setting $k = 0$ and imposing (43c). The presence of unity in the lower integration limit and the Heaviside function signifies that part of the temperature rise field behaves for short times approximately as a classical dilatational wave. For the step-stress case (45), (67) becomes

$$\frac{\pi h}{2\varepsilon} \psi \frac{\partial \theta}{\partial y} = -2 \frac{\sigma_0}{\mu} \omega_0 Q(s, x) + b_0 \omega_k S_k(s - s_0, x), \tag{69a}$$

$$Q(t, x) = \left(\int_0^t v - \int_1^t \alpha \right) S_1 I_0 \{ 2\sqrt{[\phi_0 (t - vx)]} \}\, \mathrm{d}v. \tag{69b}$$

A study of (69) shows that $\partial\theta/\partial y$ is finite as $x \to 0^+$, but singular at the dislocation edge $x = c(s - s_0)$, $s \geqslant s_0$.

The average of the gradient over the glide plane is

$$\partial\theta_0 = \frac{1}{c(s - s_0)} \int_0^{c(s-s_0)} \frac{\partial \theta}{\partial y}(x, 0, s)\, \mathrm{d}x, \quad s \geqslant s_0. \tag{70}$$

Substitution of (69) into (70), interchange of integration orders, and the use of standard tables gives a result that, in view of (52), reduces to the convenient short-time expression

$$\frac{\pi}{2} \psi \partial\theta_0 = -\frac{\varepsilon}{h} \omega_0 \frac{\sigma_0}{\mu} S_a - \left(\frac{\varepsilon}{h} \right)^2 b_0 \omega_k S_b, \tag{71}$$

where

$$S_a = \left(\int_0^\infty v - \int_1^\infty \alpha \right) S_1 I_0 [2\sqrt{(\phi_0 s)}]\, \mathrm{d}v > 0, \quad S_b = \left(\int_0^\infty v - \int_1^\infty \alpha \right) v S_1 D_k\, \mathrm{d}v > 0 \tag{72a,b}$$

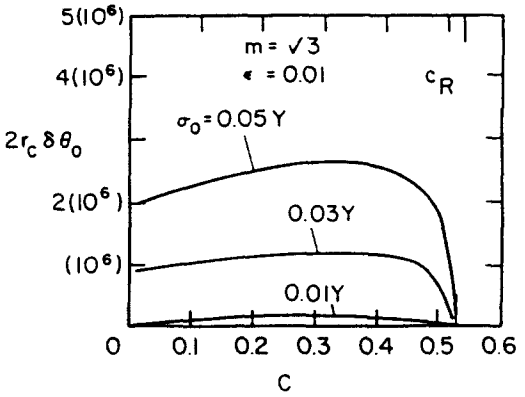

Fig. 6. Average temperature rise gradient across dislocation cut.

and D_k is again given by (54b). Equation (71) shows that, for s near s_0, the average temperature gradient has two parts: one, due to the SV-wave diffraction, is linear in the coupling constant ε, while the second part arises due to dislocation generation, and varies as the square of ε.

In view of the singular stress concentration effect of the crack edge and classical edge dislocation models, one would expect θ-variation near the dislocation cut to be extremely high, and this is borne out in Fig. 6: there, $2r_c\,\partial\theta_0$, the effective change in θ across the dislocation cut of core diameter thickness, is plotted at $s = s_0$ itself vs c for the material properties (57) and the related value

$$\psi = -8.201(10^{-5})^{\circ}\mathrm{K}^{-1}. \tag{73}$$

The curves also show order-of-magnitude variations with σ_0, and that $\partial\theta_0$ vanishes when the dislocation moves with the classical Rayleigh wave speed ($c = c_R$). This latter feature is no doubt related to the fact that the dislocation singularity order drops, as in the non-thermal case (Brock, 1982). For example, it can be shown that (46) behaves as

$$2\pi\frac{m^2}{\mu}\sigma_+ \sim \frac{b_0}{kx - s + s_0}\left(4k^2\alpha - \frac{T^2}{\beta}\right) + 2\frac{\varepsilon b_0}{h}\omega_k(S_m - kS_1)\ln\left|\frac{s - s_0}{x} - k\right| \tag{74}$$

for $x \sim c(s - s_0)$, where $(\alpha, \beta, T, S_1, S_m)$ are functions of k, and the first term in parentheses is R/β. Thus, for short times, even some purely thermal effects are sensitive to a classical phenomenon.

The large gradients, while perhaps exaggerated by the idealized, classical nature of the model, do suggest that dislocation generation is, from its onset, a potentially important source of localized material disorder (Stoltze *et al.*, 1988).

DISCUSSION

This article presented a transient 2-D analysis of edge dislocation generation near a dynamically-loaded Mode II crack in a fully-coupled thermoelastic solid. The loading was by plane SV-wave diffraction, and the dislocation moved at a constant, subcritical speed. The mixed boundary/initial value problem was solved exactly in the transform plane, and approximations to the crack plane shear stress and temperature gradient valid for short times were produced by inversion techniques.

The stress was used to study the generation process in view of a dislocation force criterion, and it was found that thermal coupling lowers, in effect, the lattice friction that the dislocation must overcome in order to move from the crack edge region. Nevertheless,

the generation, or emission time, i.e. the time between diffraction and motion, is higher than in a non-thermal analysis. However, the emitted dislocation will not, as in the non-thermal case, stop during the short time frame of the analysis.

The present results did, however, share two properties with a non-thermal study: first, the generation times were of the order of microseconds, thereby justifying the use of a semi-infinite crack and an unbounded solid. Second, the dislocation preferred, in the sense of minimum emission time, to leave the crack edge at a particular finite speed.

The Mode II dynamic stress intensity factor was also extracted, and the dislocation generation contribution was found to have an oscillatory behavior. This signifies that dislocation generation could alternatively relax and enhance the crack edge stress field, a feature not found in non-thermal studies.

In closing the analysis, the temperature gradient across the dislocation cut was found to be finite at the crack edge, and singular at the dislocation edge. Its average value over the glide plane was finite and, except at near-critical emission speeds, extremely large. This demonstrated in clear, if perhaps exaggerated fashion, the emission process potential for local material disorder through heat fluxes.

The Mode II crack-edge dislocation model used here had the advantage that the fully-coupled nature of the equations was evident, yet the problem antisymmetry rendered relatively simple emission kinematics. Of course, one consequence of antisymmetry and the associated slip but non-opening of the crack faces was a crack plane of zero temperature rise. On the other hand, the very fact that the thermal effects revealed were distinctive suggests that they would be at least equally so in a more general loading situation with crack plane temperature rises.

On the same note, this analysis was a straightforward application of the fully-coupled equations to classical dislocation motion; no attempt was made to impose a heat source at the dislocation edge, say. Again, the fact that the resulting thermal effects were distinctive suggests that dislocation generation processes may be more accurately described by a thermal analysis. Indeed, for short times a thermal analysis is perhaps warranted for crack edge process zones, even when fully plastic effects have not arisen.

The use of the classical dislocation (Love, 1944) produces, of course, severely singular behavior when the dislocation and crack edges coincide. Following preliminary efforts by Wu and Brock (1987), future emission studies will make use of dislocation distributions. The 2-D nature of the analysis also idealized the generation kinematics; it is known [e.g. Panfilov *et al.* (1990)] that dislocation and crack edges are not necessarily parallel. The present analysis was, however, a first step, and attempted to provide qualitative results with a minimum of parameters. Moreover, it allowed insight into the role of thermal effects by comparison with existing 2-D classical dislocation-based results—both quasi-static and transient.

In closing, it should also be noted that, in the course of the analysis, an exact expression for the classical non-thermal Rayleigh wave speed as a zero of the Rayleigh function was obtained, as well as a useful approximation for zeroes of the corresponding thermoelastic Rayleigh function in the transform plane. However, the function arose from the anti-symmetry-based conditions of specified stress and zero temperature rise on a surface. A surface with other temperature conditions would, of course, provide a different thermoelastic Rayleigh function [e.g. Chadwick (1960)].

Acknowledgement—This research was supported by NSF Grant MSM 8917944.

REFERENCES

Abramowitz, M. and Stegun, I. A. (1964). *Handbook of Mathematical Functions*. Dover, New York.
Achenbach, J. D. (1973). *Wave Propagation in Elastic Solids*. North-Holland, Amsterdam.
Boley, B. and Tolins, I. S. (1962). Transient coupled thermoelastic boundary-value problems in the half-plane. *ASME J. Appl. Mech.* **29**, 637–646.
Boley, B. and Weiner, J. H. (1960). *Theory of Thermal Stresses*. Wiley, New York.
Brock, L. M. (1982). Dynamic solution for the non-uniform motion of an edge dislocation. *Int. J. Engng Sci.* **20**, 113–118.

Brock, L. M. (1989a). An exact transient analysis of dislocation emission and fracture. *J. Mech. Phys. Solids* **37**, 47–69.

Brock, L. M. (1989b). Transient analyses of dislocation emission in the three modes of fracture. *Int. J. Engng Sci.* **27**, 1479–1495.

Brock, L. M., Matic, P. and DeGiorgi, V. G. (1992). Early transient response during crack propagation in a weakly-coupled thermoelastic solid. *Int. J. Solids Structures* **29**(8), 973–989.

Brock, L. M. and Thomas, J. P. (1992). Thermal effects in rudimentary crack edge inelastic zone growth under stress wave loading. *Acta Mech.* (accepted).

Brock, L. M. and Wu, J.-S. (1990a). Incident wave and dislocation acceleration effects in dislocation emission from cracks. *ASME J. Appl. Mech.* **57**, 870–876.

Brock, L. M. and Wu, J.-S. (1990b). Transient studies of screw and edge dislocation generation at crack edges. *J. Elasticity* **24**, 187–209.

Carrier, G. F. and Pearson, C. E. (1988). *Partial Differential Equations* (2nd Edn). Academic Press, New York.

Chadwick, P. (1960). Thermoelasticity, the dynamical theory. In *Progress in Solid Mechanics* (Edited by I. N. Sneddon and R. Hill), Vol. 1. North-Holland, Amsterdam.

Gradshteyn, I. S. and Ryzhik, I. MN. (1980). *Table of Integrals, Series and Products*. Academic Press, New York.

Johnston, W. G. and Gilman, J. J. (1959). Dislocation velocities, dislocation densities, and plastic flow in lithium fluoride crystals. *J. Appl. Phys.* **30**, 129–144.

Love, A. E. H. (1944). *A Treatise on the Mathematical Theory of Elasticity* (4th Edn). Dover, New York.

Majumdar, B. S. and Burns, S. J. (1981). An elastic theory of dislocations, dislocation arrays, and inclusions near a sharp crack. *Acta Metall.* **29**, 579–588.

Mura, T. (1982). *Micromechanics of Defects in Solids*. Martinus Nijhoff, The Hague.

Noble, B. (1958). *Methods Based on the Wiener–Hopf Technique*. Pergamon Press, New York.

Ohr, S. M. (1985). An electron microscope study of crack tip deformation and its impact on the dislocation theory of fracture. *Mater. Sci. Engng* **72**, 1–35.

Panfilov, P., Yermakov, A. and Baturin, G. (1990). The cause of cleavage in iridium single crystals. *J. Mater. Sci. Lett.* **9**, 1162–1164.

Rice, J. R. and Thomson, R. (1974). Ductile versus brittle behavior of crystals. *Phil. Mag.* **29**, 73–97.

Shaw, M. C. (1984). A critical review of mechanical failure criteria. *ASME J. Engng Mater Tech.* **106**, 219–226.

Sneddon, I. N. (1972). *The Use of Integral Transforms*. McGraw-Hill, New York.

Stoltze, P., Norskov, J. K. and Landman, U. (1988). Disordering and melting of aluminum surfaces. *Phys. Rev. Lett.* **61**, 440–443.

Taylor, G. I. (1934). The mechanism of plastic deformation of crystals. *Proc. R. Soc.* **A145**, 362–415.

Taylor, G. I. and Quinney, M. A. (1934). The latent energy remaining in a metal after cold working. *Proc. R. Soc.* **A143**, 307–322.

Weichert, R. and Schonert, K. (1974). On the temperature rise at the tip of a fast-running crack. *J. Mech. Phys. Solids* **22**, 127–133.

Wu, J.-S. and Brock, L. M. (1987). Transient analysis of dislocation emission by a crack using a modified dislocation model. In *Developments in Mechanics*. (Edited by W. Soedel and J. F. Hamilton), Vol. 14b. Purdue University, West Lafayette, IN.

Zehnder, A. T. and Rosakis, A. (1991). On the temperature distribution at the vicinity of dynamically propagating cracks in 4340 steel. *J. Mech. Phys. Solids* **39**, 385–415.